Mon. Not. R. Astron. Soc. **398,** 2143–2151 (2009) doi:10.1111/j.1365-2966.2009.15264.x

Halo abundances in the $f_{\rm nl}$ model

Tsz Yan Lam★ and Ravi K. Sheth★

Center for Particle Cosmology, University of Pennsylvania, 209 S. 33rd Street, Philadelphia, PA 19104, USA

Accepted 2009 June 17. Received 2009 June 10; in original form 2009 May 11

ABSTRACT

We show how the excursion set moving barrier model for halo abundances may be generalized to the local non-Gaussian $f_{\rm nl}$ model. Our estimate assumes that the distribution of step sizes depends on $f_{\rm nl}$, but that they are otherwise uncorrelated. Our analysis is consistent with previous results for the case of a constant barrier, and highlights some implicit assumptions. It also clarifies the basis of an approximate analytic solution to the moving barrier problem in the Gaussian case, and shows how it might be improved.

Key words: methods: analytical – large-scale structure of Universe.

1 INTRODUCTION

Detections of non-Gaussianity can discriminate between different inflation models (e.g. Maldacena 2003). The local $f_{\rm nl}$ model, where the primordial perturbation potential is

$$\Phi = \phi + f_{\rm nl}(\phi^2 - \langle\phi^2\rangle), \tag{1}$$

where ϕ is a Gaussian potential field and $f_{\rm nl}$ is a scalar, has been the subject of much recent study (e.g. Buchbinder, Khoury & Ovrut 2008; Khoury & Piazza 2008; Silvestri & Trodden 2008, and references therein). Constraints on this model tend to be of two types – from the CMB (Hikage et al. 2008; McEwen et al. 2008; Yadav & Wandelt 2008; Komatsu et al. 2009) and from large-scale structures in the Universe (Koyama, Soda & Taruya 1999; Matarrese, Verde & Jimenez 2000; Scoccimarro, Sefusatti & Zaldarriaga 2004; Izumi & Soda 2007; Sefusatti & Komatsu 2007; Afshordi & Tolley 2008; Carbone, Verde & Matarrese 2008; Dalal et al. 2008; Desjacques, Seljak & Iliev 2008; Grossi et al. 2008; Lo Verde et al. 2008; McDonald 2008; Matarrese & Verde 2008; Slosar et al. 2008; Slosar 2008; Taruya, Koyama & Matsubara 2008; Grossi et al. 2009; Kamionkowski, Verde & Jimenez 2009; Lam & Sheth 2009; Valageas 2009).

One of the fundamental quantities of interest in such studies is the abundance of virialized dark matter haloes. Press & Schechter (1974) suggested that the abundance of collapsed virialized haloes may be estimated from the statistics of the initial fluctuation field. They used the assumption that haloes form from a spherical collapse to argue that such objects started out as sufficiently overdense regions in the initial fluctuation field. The excursion set approach of Bond et al. (1991) allows one to estimate halo abundances in Gaussian theories; in this context, the spherical collapse model is associated a barrier of constant height. If the collapse is triaxial then the barrier height is stochastic with a mean that is not constant (Sheth, Mo & Tormen 2001). Ignoring the stochasticity but including the changing of the barrier height allows the excursion set approach to provide a simple parametrization of the effects of triaxial collapse on halo abundances (Sheth & Tormen 2002). The main goal of the present work is to show how to generalize the moving barrier formulae of Sheth & Tormen (2002) to the local non-Gaussian $f_{\rm nl}$ model.

Section 2 provides explicit expressions for the one- and two-point distribution of the overdensity in $f_{\rm nl}$ models. These are used, in Section 3, to estimate how the mass function of virialized objects is modified when $f_{\rm nl} \neq 0$. This section also clarifies earlier work on the Gaussian ($f_{\rm nl} = 0$) case. A final section summarizes our results. Two appendices provide useful approximations and other technical details.

2 THE LOCAL NON-GAUSSIAN MODEL

We are interested in models where the primordial perturbation potential is given by equation (1). We will use $P_\phi(k)$ to represent the power spectrum of ϕ; in what follows, we will set $P_\phi(k) = Ak^{n_s-4}$, where $n_s \approx 1$ and A is a normalization constant that is fixed by requiring that the rms fluctuation in the associated non-Gaussian initial density field (which we will define shortly) has value σ_8. The power spectrum and bispectrum of the Φ field are

$$P_\Phi(k) = P_\phi(k) + \frac{2f_{\rm nl}^2}{(2\pi)^3}\int {\rm d}\boldsymbol{q}[P_\phi(q)P_\phi(|\boldsymbol{k}-\boldsymbol{q}|) - P_\phi(k)P_\phi(q) - P_\phi(k)P_\phi(|\boldsymbol{k}-\boldsymbol{q}|)], \tag{2}$$

★E-mail: tszylam@gmail.com (TYL); shethrk@physics.upenn.edu (RKS)

$$B_\Phi(k_1, k_2, k_{12}) \equiv 2 f_{\rm nl} \left[P_\phi(k_1)P_\phi(k_2) + {\rm cyclic}\right] + \mathcal{O}\left(f_{\rm nl}^3\right) \tag{3}$$

(Scoccimarro et al. 2004).

Most of the complication in $f_{\rm nl}$ models arises from the fact that we are almost always interested in spatially smoothed quantities. In particular, the quantity $\sigma S_3 \equiv \langle\delta^3|R\rangle/\langle\delta^2|R\rangle^{3/2}$ will play an important role, because it represents the leading order contribution to the non-Gaussianity (note that it is proportional to $f_{\rm nl}$). Fortunately, smoothing is a linear operation, so the smoothed variables are just linear combinations of the unsmoothed ones. Hence, if $W(kR)$ denotes the Fourier transform of the smoothing window of scale R then, to second order in $f_{\rm nl}$,

$$\langle\delta^2|R\rangle = \sigma^2(R) = \frac{1}{(2\pi)^3}\int \frac{{\rm d}k}{k} 4\pi k^7 M^2(k)\, P_\Phi(k)\, W^2(kR) \qquad \text{and} \tag{4}$$

$$\langle\delta^3|R\rangle = 2 f_{\rm nl}\,\frac{2}{(2\pi)^4}\int \frac{{\rm d}k_1}{k_1} k_1^5 M(k_1)W(k_1R)\int \frac{{\rm d}k_2}{k_2} k_2^5 M(k_2)W(k_2R)\int {\rm d}\mu_{12}\, k_{12}^2\, M(k_{12})W(k_{12}R)\frac{B_\Phi(k_1,k_2,k_{12})}{2f_{\rm nl}}, \tag{5}$$

where $M(k) \equiv [3D(z)c^2]/(5\Omega_{\rm m}H_0^2)\,T(k)$, $T(k)$ is the cold dark matter transfer function and $D(z)$ is the linear growth function. In hierarchical models, σ and σS_3 are both monotonically decreasing functions of R; this will be important in what follows. Appendix 5 provides a useful fitting formula for $\sigma\ S_3$, and shows that it is only a weak function of scale.

2.1 Edgeworth approximations for $p(\delta|R)$ and $p(\delta,\ \Delta|r,\ R)$

Because we are interested in small departures from Gaussianity, the Edgeworth expansion provides a convenient form for the distribution of δ smoothed on scale R:

$$p(\delta|R)\,{\rm d}\delta \approx \left\{1 + \frac{\sigma(R)S_3(R)}{6}H_3\left[\frac{\delta}{\sigma(R)}\right]\right\}\frac{{\rm e}^{-\delta^2/2\sigma^2(R)}}{\sqrt{2\pi}\sigma(R)}\,{\rm d}\delta = \left[1 + \frac{\sigma S_3}{6}H_3(\nu)\right]\ p_0(\delta|R)\,{\rm d}\delta, \tag{6}$$

where $\sigma(R)$ is given by equation (4), $\sigma S_3 \equiv \langle x^3\rangle/\langle x^2\rangle^{3/2} = 2 f_{\rm nl}\gamma^3/\sigma^3$, and $H_3(\nu) \equiv \nu(\nu^2-3)$ with $\nu \equiv \delta/\sigma(R)$. Because H_3 changes sign at $\nu = \sqrt{3}$, the Edgeworth expansion is not always positive, making it ill suited for studying (at least one of) the tails of the distribution. The expansion becomes negative when $(\sigma S_3/6)\nu(\nu^2-3) = -1$, meaning $\nu(\nu^2-3) = -200\,(0.03/\sigma S_3)$, and note that σS_3 has the opposite sign to $f_{\rm nl}$. For $f_{\rm nl} \approx 100$, we have $\nu(\nu^2-3) = 200$, so there certainly are problems at $\nu > 6$, making the expansion suspect at slightly smaller values. For $f_{\rm nl} \approx -100$, there are problems at $\nu < -6$. Because the Gaussian piece falls exponentially with ν^2, the fact that the expansion may not be accurate at large ν may not matter – but, for larger $|f_{\rm nl}|$ values this limitation of the Edgeworth approach should be borne in mind.

Lam & Sheth (2009) have used this expansion in the context of modelling the one-point distribution of the evolved non-linear δ, where σS_3 is smaller and large ν values are indeed rare. Here, however, we will follow Lo Verde et al. (2008), and use it in our model of halo abundances. In this case, it is the large ν tail which is of most interest, and this is precisely where the Edgeworth expansion is most suspect. However, note that, when modelling haloes, one is most interested in the regime where $\nu > 0$, so, for $f_{\rm nl} < 0$, the Edgeworth expansion is positive definite except for large σS_3, for which we know the Edgeworth expansion is not useful anyway. In any case, Appendix 5 shows that large values of σS_3 are not currently a concern.

For reasons that will become clear shortly, we will also be interested in the value of the field when it is smoothed on two different scales. For small departures from Gaussianity, the bivariate Edgeworth expansion should provide a good description. It is

$$p(\mu,\nu) = \frac{1}{2\pi\sqrt{1-q^2}}\exp\left[-\frac{\mu^2 - 2q\mu\nu + \nu^2}{2(1-q^2)}\right]\left[1 + \frac{\lambda_{30}H_{30} + \lambda_{03}H_{03}}{6} + \frac{\lambda_{21}H_{21} + \lambda_{12}H_{12}}{2}\right] \tag{7}$$

(Kotz, Balakrishnan & Johnson 2000), where

$$\mu \equiv \frac{\delta}{\langle\delta^2\rangle^{1/2}},\quad \nu \equiv \frac{\Delta}{\langle\Delta^2\rangle^{1/2}},\quad q \equiv \langle\mu\,\nu\rangle,\quad \lambda_{mn} = \langle\mu^m\nu^n\rangle_c \quad \text{and} \quad H_{mn}(\mu,\nu,q) = \frac{h_{mn}(\mu,\nu,q)}{(1-q^2)^2},$$

with

$$h_{30}(\mu,\nu,q) = h_{03}(\nu,\mu,q) = \frac{(\mu - q\nu)^3}{1-q^2} - 3(\mu - q\nu),$$

$$h_{21}(\mu,\nu,q) = h_{12}(\nu,\mu,q) = 2q(\mu - q\nu) - (\nu - q\mu) + \frac{(\nu - q\mu)(\mu - q\nu)^2}{1-q^2}.$$

If our convention is that Δ is the field on the larger smoothing scale, then, to lowest order in $\lambda_{03} = \sigma S_3$,

$$p(\mu|\nu) = \frac{1}{\sqrt{2\pi(1-q^2)}}\exp\left[-\frac{(\mu - q\nu)^2}{2(1-q^2)}\right]\left[1 + \frac{\lambda_{30}H_{30} + \lambda_{03}H_{03}}{6} + \frac{\lambda_{21}H_{21} + \lambda_{12}H_{12}}{2} - \frac{\lambda_{03}H_3(\nu)}{6}\right]. \tag{8}$$

In what follows, we will set $q^2 = \langle\Delta^2\rangle/\langle\delta^2\rangle$ (as it is for a Gaussian field smoothed with a top hat in k-space; this is standard for the excursion set approach).

3 HALO ABUNDANCES

Recall that σ is a monotonically decreasing function of smoothing scale R. In the initial conditions, where fluctuations are negligible, the smoothing scale R contains mass $m = \bar{\rho}\, 4\pi R^3/3$ almost surely, so σ, R and m are equivalent variables. Now, let $\mathrm{d}n/\mathrm{d}m$ denote the comoving number density of haloes of mass m and $\bar{\rho}$ denote the comoving density of the background. If $f(m)$ denotes the mass fraction in haloes of mass m then

$$F\{<\sigma[R=(3m/4\pi\bar{\rho})^{1/3}]\} = F(>m) = \int_m^\infty \mathrm{d}m\, f(m) = \int_m^\infty \frac{\mathrm{d}m}{\bar{\rho}}\,\frac{\mathrm{d}n(m)}{\mathrm{d}\ln m}. \tag{9}$$

An estimate of F, then, is an estimate of $\mathrm{d}n/\mathrm{d}\ln m$. The following sections describe the excursion set estimate of F for Gaussian initial conditions, and how this estimate can be extended to the $f_{\rm nl} \neq 0$ models.

3.1 Excursion set approach

The excursion set approach (Bond et al. 1991; Lacey & Cole 1993; Sheth 1998) relates the number of haloes of mass m to the first crossing of a suitably chosen barrier $b(\sigma)$ by a suitably chosen set of walks. The simplest implementations of this approach consider the first crossing of $b(\sigma)$ by an ensemble of uncorrelated random walks with uncorrelated steps. While neglecting both types of correlations is far from ideal, previous work shows that this allows one to write down simple analytic expressions for the first crossing distribution and how this distribution is related to halo abundances, which together provide reasonably accurate descriptions of halo abundances as well as their formation histories.

The barrier shape $b(\sigma)$ is set by the physics of collapse. The spherical collapse model has a barrier of constant height $b(\sigma) = \delta_{\rm sc}$, whereas barriers of the form

$$b(\sigma) = \sqrt{a}\delta_c\left[1+\beta\,(\sigma/\sqrt{a}\delta_c)^{2\gamma}\right], \tag{10}$$

with $\beta = 0.4$ and $\gamma = 0.6$, may be related to models in which haloes form from a triaxial collapse (Sheth et al. 2001; Sheth & Tormen 2002). The physics of collapse have $a = 1$, but setting $a = 0.7$ results in a predicted $\mathrm{d}n/\mathrm{d}\ln m$ which is in much better agreement with the abundance observed in simulations (see Sheth et al. 2001, for further discussion of why $a \neq 1$).

3.2 The Gaussian case: spherical collapse

Let $p(\delta, s)$ denote the probability that a randomly placed cell in the initial distribution has overdensity δ when the smoothing scale is such that $\langle\delta^2\rangle = \sigma^2 \equiv s$. Classify all cells by the largest scale $S \leq s$ on which they had overdensity greater than δ_c. Then, provided $\delta \geq \delta_c$,

$$p(\delta, s) = \int_0^s \mathrm{d}S\, f(S, \delta_c)\, p(\delta, s|\delta_c, S, \mathrm{first}), \tag{11}$$

where f is the fraction of cells for which S was the largest smoothing scale on which the overdensity was greater than δ_c and $p(\delta, s|\delta_c, S, \mathrm{first})$ is the probability that the overdensity on scale s is δ given that S was the largest scale on which the overdensity exceeded δ_c. If one views a plot of δ versus smoothing scale as something which resembles a random walk, with large smoothing scales to the left, then S is the first 'time' that the walk crosses δ_c: hence, the word 'first' in the expression above. Therefore,

$$P(\delta_c, s) \equiv \int_{\delta_c}^\infty \mathrm{d}\delta\, p(\delta, s) = \int_0^s \mathrm{d}S\, f(S, \delta_c) \int_{\delta_c}^\infty \mathrm{d}\delta\, p(\delta, s|\delta_c, S, \mathrm{first}) = \int_0^s \mathrm{d}S\, f(S, \delta_c)\, P(\delta_c, s|\delta_c, S, \mathrm{first}). \tag{12}$$

In what follows, we will use the subscript '0' to denote quantities associated with Gaussian initial conditions (for which $f_{\rm nl} = 0$). For a Gaussian field smoothed with a top hat in k-space,

$$p_0(\delta_1, s|\delta_2, S, \mathrm{first}) = p_0(\delta_1, s|\delta_2, S) = p_0(\delta_1 - \delta_2, s - S), \tag{13}$$

so $P_0(\delta_c, s|\delta_c, S, \mathrm{first}) = P_0(0, s - S) = 1/2$, and equation (12) implies

$$P_0(\delta_c, s) \equiv \int_{\delta_c}^\infty \mathrm{d}\delta\, p_0(\delta, s) = \int_0^s \mathrm{d}S\, \frac{f_0(S, \delta_c)}{2} \equiv \frac{F_0(<s)}{2} = \frac{F_0(>m)}{2}. \tag{14}$$

Differentiating both sides with respect to s shows that f_0 is simply related to p_0:

$$\frac{\partial P_0}{\partial s} = -p_0\left(\frac{\delta_c}{\sqrt{s}}\right)\frac{\partial(\delta_c/\sqrt{s})}{\partial s} = \frac{\delta_c}{2s^{3/2}}\frac{\mathrm{e}^{-\delta_c^2/2s}}{\sqrt{2\pi}} = \frac{f_0(s, \delta_c)}{2}. \tag{15}$$

3.3 The Gaussian case: ellipsoidal collapse

If δ_c depends on s, as in some parametrizations of triaxial collapse, then this simplicity is lost. In particular, for the barrier given in equation (10), Sheth & Tormen (2002) show that

$$s f_0(s, b) \approx \frac{b(0)}{\sqrt{2\pi s}}\exp\left(-\frac{b^2}{2s}\right)\left[1 + 0.067\,\frac{s^\gamma}{\left(a\delta_c^2\right)^\gamma}\right]. \tag{16}$$

To see where this comes from, note that the analogue of equation (14) becomes

$$\frac{\partial P_0}{\partial s} = -\frac{\mathrm{e}^{-b^2/2s}}{\sqrt{2\pi s}}\left[\frac{\partial b}{\partial s} - \frac{b}{2s}\right] = \frac{f_0(s,b)}{2} - \int_0^s \mathrm{d}S\, f_0(S,B)\,\frac{\mathrm{e}^{-(b-B)^2/2(s-S)}}{\sqrt{2\pi(s-S)}}\left[\frac{\partial b}{\partial s} - \frac{(b-B)}{2(s-S)}\right]. \tag{17}$$

However, the first term in square brackets on the right-hand side is independent of S, so this term integrates to $p(b,s)\,\partial b/\partial s$. Since there is a similar term on the left-hand side, this leaves

$$\frac{b}{s}\frac{\mathrm{e}^{-b^2/2s}}{\sqrt{2\pi s}} = f_0(s,b) + \int_0^s \mathrm{d}S\, f_0(S,B)\,\frac{\mathrm{e}^{-(b-B)^2/2(s-S)}}{\sqrt{2\pi(s-S)}}\frac{(b-B)}{(s-S)}. \tag{18}$$

where we have multiplied both sides by a factor of 2. Writing $B(S)$ as a Taylor series around $b(s)$ implies

$$\frac{b}{s}\frac{\mathrm{e}^{-b^2/2s}}{\sqrt{2\pi s}} = f_0(s,b) + \sum_{i=1}^{\infty}\frac{\partial^i b}{\partial s^i}\int_0^s \mathrm{d}S\, f_0(S,B)\,\frac{\mathrm{e}^{-(b-B)^2/2(s-S)}}{\sqrt{2\pi(s-S)}}\frac{(S-s)^{i-1}}{i!}. \tag{19}$$

so

$$s f_0(s,b) = \left(b - s\frac{\partial b}{\partial s}\right)\frac{\mathrm{e}^{-b^2/2s}}{\sqrt{2\pi s}} - \sum_{i=2}^{\infty}\frac{s^i}{i!}\frac{\partial^i b}{\partial s^i}\int_0^s \mathrm{d}S\, f_0(S,B)\,\frac{\mathrm{e}^{-(b-B)^2/2(s-S)}}{\sqrt{2\pi(s-S)}}(S/s-1)^{i-1}. \tag{20}$$

Equation (16), the approximation of Sheth & Tormen (2002), corresponds to ignoring all S/s terms and then keeping only the first few terms in the series.

3.4 Dependence on $f_{\rm nl}$

We now extend the analysis above to the case in which $f_{\rm nl} \neq 0$. Our primary assumption is that the expressions above remain valid if p on the left-hand side of equation (12) is given by the Edgeworth expansion, and the conditional distribution on the right-hand side is given by the bivariate Edgeworth expansion. This is not quite right, since the steps in the walk are now correlated, and we are assuming that the statistics of walking from (B, S) to (B, S) do not depend on the fact that the walk did not cross B before S. In effect, this means that we assume that the extra constraint that $\delta' < \delta_c$ for all $S' < S$ makes no difference, so the only difference from the Gaussian calculation is that all probability density functions (PDFs) are now replaced by the appropriate Edgeworth approximation.

To see what this implies, it is convenient to first define

$$\mathcal{G}_{\rm mn} = \int_0^{\infty}\mathrm{d}\delta\, p_0(\delta+b, s|B, S)h_{\rm mn}\left(\frac{\delta+b}{\sqrt{s}}, \frac{B}{\sqrt{S}}, \sqrt{\frac{S}{s}}\right), \tag{21}$$

where

$$\begin{aligned}
\mathcal{G}_{30} &= -\frac{\sqrt{s-S}}{\sqrt{s}}\left[1 - \frac{(b-B)^2}{s-S}\right]p_0\left(\frac{b-B}{\sqrt{s-S}}\right)\\
\mathcal{G}_{03} &= \frac{(s-S)^2}{s^2}H_3(B/\sqrt{S})P_0\left(\frac{b-B}{\sqrt{(s-S)}}\right)\\
&\quad -\frac{1}{s^2\sqrt{S}\sqrt{s-S}}\left\{S(s-S)(2S-3s) + [S^2(b^2+bB+B^2) - 3sS(bB+B^2) + 3B^2s^2]\right\}p_0\left(\frac{b-B}{\sqrt{s-S}}\right)\\
\mathcal{G}_{21} &= \frac{\sqrt{S}\sqrt{s-S}}{s}\left[1 - \frac{(b-B)^2}{s-S} + \frac{B(b-B)}{S}\right]p_0\left(\frac{b-B}{\sqrt{s-S}}\right)\\
\mathcal{G}_{12} &= \frac{-sS(s-S) + (bS-Bs)^2}{Ss^{3/2}\sqrt{s-S}}p_0\left(\frac{b-B}{\sqrt{s-S}}\right).
\end{aligned} \tag{22}$$

In addition, define

$$\mathcal{G}_3 \equiv \int_0^{\infty}\mathrm{d}\delta\, p_0(\delta+b, s|B, S)H_3(B/\sqrt{S}) = H_3(B/\sqrt{S})P_0\left(\frac{b-B}{\sqrt{s-S}}\right). \tag{23}$$

If we ignore the scale dependence of σS_3 (Fig. 1 shows that it is weak) then the derivative of equation (12) w.r.t. s is

$$\frac{\partial P_0(b/\sqrt{s})}{\partial s}\left[1 + \frac{\sigma S_3}{6}H_3\left(\frac{b}{\sqrt{s}}\right)\right] = \frac{f(s,b)}{2} + \int_0^s \mathrm{d}S\, f(S,B)\frac{\partial}{\partial s}P_0\left(\frac{b-B}{\sqrt{s-S}}\right) + \frac{\sigma S_3}{6}\int_0^s \mathrm{d}S\, f(S,B)\frac{\partial}{\partial s}\left[\mathcal{E}(s,S)p_0\left(\frac{b-B}{\sqrt{s-S}}\right)\right], \tag{24}$$

where

$$\mathcal{E}(s,S) = \frac{-4s^{3/2} + 6s\sqrt{S} - 2S^{3/2}}{(s-S)^{3/2}} + \frac{3B\sqrt{s-S}}{S(\sqrt{s}+\sqrt{S})^2}(B\sqrt{s} + b\sqrt{S}) + \frac{(b-B)^2\sqrt{s-S}}{(\sqrt{s}+\sqrt{S})^3}. \tag{25}$$

Note that, in contrast to the case in which $f_{\rm nl} = 0$, the final term on the right-hand side of equation (24) is non-trivial because it is now s dependent.

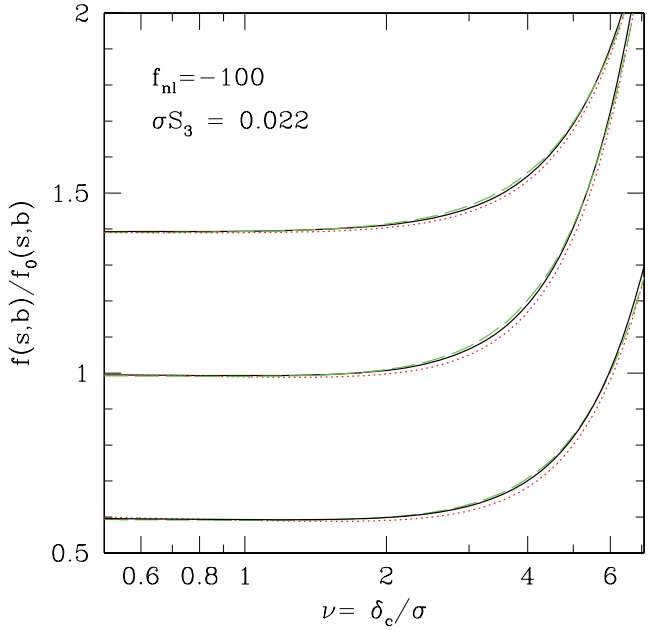

Figure 1. Ratio of the first crossing probability for $f_{\rm nl} = -100$ to that when $f_{\rm nl} = 0$. Solid (black) curves set $\sigma S_3 = 0.022$ and $\mathcal{G}(s, b) = 0$, dotted (red) curves include $\mathcal{G}(s, b) \neq 0$ but keep σS_3 fixed and the dashed (green) curves include the scale dependence of σS_3 but set $\mathcal{G}(s, b) = 0$. The top set of curves (offset upwards by 0.4) show results for a moving barrier (equation 10), middle curves use a constant barrier with $\delta_c = 1.66$ and lowest curves (offset downwards by 0.4) use a constant barrier of height $\sqrt{0.7}\delta_c$.

Substituting the $f_{\rm nl} = 0$ solution for the pieces with subscript '0' yields

$$\frac{f_0(s,b)}{2}\left[1+\frac{\sigma S_3}{6}H_3\left(\frac{b}{\sqrt{s}}\right)\right] = \frac{f(s,b)}{2}\left\{1+2\int_0^s \mathrm{d}S\,\frac{\partial}{\partial s}P_0\left(\frac{b-B}{\sqrt{s-S}}\right)\frac{f(S,B)-f_0(S,B)[1+(\sigma S_3/6)H_3(b/\sqrt{s})]}{f(s,b)} + 2\frac{\sigma S_3}{6}\int_0^s \mathrm{d}S\,\frac{f(S,B)}{f(s,b)}\frac{\partial}{\partial s}\left[\mathcal{E}(s,S)p_0\left(\frac{b-B}{\sqrt{s-S}}\right)\right]\right\}. \quad (26)$$

This is an integral equation for $f(s, b)$ which is valid when $f_{\rm nl} \neq 0$. Clearly, the zeroth-order solution is simply the $f_{\rm nl} = 0$ solution (the Gaussian case) times a correction term which depends on σS_3 and the barrier shape $b(s)$. We can include the next-to-leading order contribution as

$$f(s,b) = f^{(0)}(s,b)\left[1+\frac{f^{(1)}}{f^{(0)}}\right] = f_0(s,b)\left[1+\frac{\sigma S_3}{6}H_3\left(\frac{b}{\sqrt{s}}\right)\right]\left[1-\frac{\sigma S_3}{6}\mathcal{G}(s,b)\right], \quad (27)$$

where f_0 is the first crossing probability associated with uncorrelated steps when $f_{\rm nl} = 0$ (approximated by equation 16),

$$\mathcal{G}(s,b) = 2\int_0^s \mathrm{d}S\,\frac{f_0(S,B)}{f_0(s,b)}\left\{\frac{\partial}{\partial s}\left[\mathcal{E}(s,S)p_0\left(\frac{b-B}{\sqrt{s-S}}\right)\right]+\frac{\partial}{\partial s}P_0\left(\frac{b-B}{\sqrt{s-S}}\right)[H_3(B/\sqrt{S})-H_3(b/\sqrt{s})]\right\}, \quad (28)$$

where only terms to first order in σS_3 have been kept, and

$$\frac{\partial\mathcal{E}}{\partial s} = \frac{-3\sqrt{S}}{\sqrt{s-S}(\sqrt{s}+\sqrt{S})^2}+\frac{3B}{S\sqrt{s-S}(\sqrt{s}+\sqrt{S})}\left[\frac{3B(\sqrt{s}-\sqrt{S})}{2\sqrt{s}}+(B+b)\sqrt{\frac{S}{s}}+\sqrt{S}\frac{\partial b}{\partial s}(\sqrt{s}-\sqrt{S})\right] - \frac{9B}{2S\sqrt{s-S}(\sqrt{s}+\sqrt{S})^2}\left(B\sqrt{s}+b\sqrt{S}\right)+\frac{b-B}{\sqrt{s-S}(\sqrt{s}+\sqrt{S})^3}\left[2(s-S)\frac{\partial b}{\partial s}+\frac{b-B}{2}\right]-\frac{3}{2}\frac{(b-B)^2\sqrt{s-S}}{\sqrt{s}(\sqrt{s}+\sqrt{S})^4}. \quad (29)$$

Thus,

$$f(s,b) \approx f_0(s,b)\left[1+\frac{\sigma S_3}{6}H_3\left(\frac{b}{\sqrt{s}}\right)-\frac{\sigma S_3}{6}\mathcal{G}(s,b)\right]. \quad (30)$$

The analysis simplifies somewhat for a constant barrier (see Appendix 6). Previous analyses of the case in which the barrier is a constant either have explicitly ignored the final term in the square brackets above (Matarrese et al. 2000) or have missed the fact that it is there entirely (Lo Verde et al. 2008).

Fig. 1 shows the effect of $\mathcal{G}(s, b)$ on the ratio of the first crossing distribution when $f_{\rm nl} = -100$ to that when $f_{\rm nl} = 0$. This is done for three different barriers: the top curves (offset upwards by 0.4) show results for the moving barrier of equation (10), the middle are for a constant barrier of height $b = \delta_c$ and the lowest (offset downwards by 0.4) for $b = \sqrt{0.7}\delta_c$. The middle curves are for the barrier shape that has been previously studied (Matarrese et al. 2000; Lo Verde et al. 2008); differences between these and the bottom curves are due to the barrier height. Differences between the top and bottom sets of curves are due to the s dependence of the barrier.

In each case, the black (solid) curves show the result of neglecting the factor of $\mathcal{G}(s)$ and setting $\sigma S_3 = 0.022$ (i.e. we ignore the fact that it depends weakly on scale). The red (dotted) curves include the fact that $\mathcal{G}(s, b) \neq 0$ [or the corresponding $G(s)$ (equation B8) for

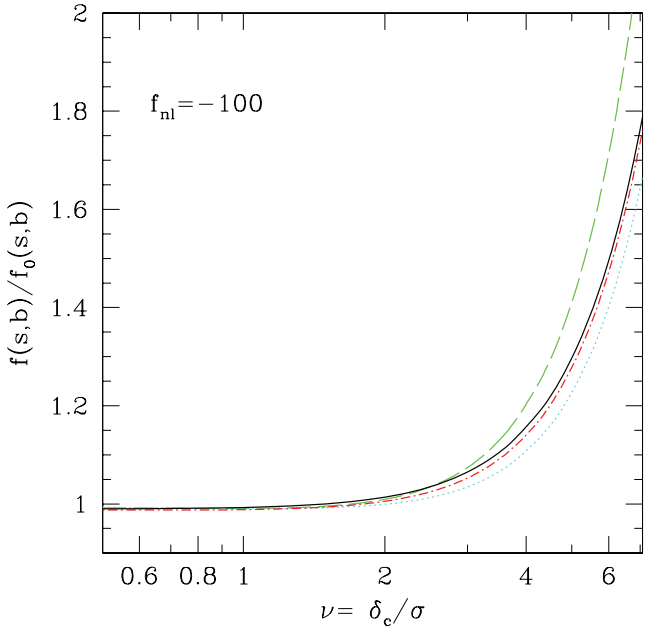

Figure 2. Ratios of the first crossing probability for $f_{\rm nl} = -100$ to that when $f_{\rm nl} = 0$. Black (solid), green (dashed) and cyan (dotted) curves plot the ratios for moving barrier $b(s)$, $b = \delta_c$ and $b = \sqrt{0.7}\delta_c$ when $\mathcal{G}(s)$ is set to 0. The red (dot–dashed) curve shows equation (30).

the constant barrier] with the same (fixed) value of σS_3. The differences between these two sets of curves are small for all three barriers, indicating that the contribution from the factor $\mathcal{G}$ is small. The effect of again ignoring $\mathcal{G}$, but now including the scale dependence of σS_3 (using equation A1), but setting $\partial\sigma S_3/\partial s \approx 0$ is shown by the green (dashed) curves.

Fig. 2 shows the ratios of the first crossing distribution for different barrier shapes. The scale dependence of σS_3 is included and computed by the approximation formula (equation A1). Black (solid), green (dashed) and cyan (dotted) curves plot the ratios for moving barrier $b(s)$, $b = \delta_c$ and $b = \sqrt{0.7}\delta_c$, respectively (all without $\mathcal{G}$). The red (dot–dashed) curve shows the term in square brackets in equation (30): this includes the scale dependence in the factor σS_3 but it sets $\partial \ln \sigma S_3/\partial\, s \approx 0$, and it ignores the fact that this scale dependence will also modify the $\mathcal{G}(s, b)$ term. The inclusion of the factor $\mathcal{G}(s, b)$ has a small effect compared to using different barrier shapes. The three barrier shapes result in slightly different predictions for how $f_{\rm nl}$ modifies halo abundances. Therefore, comparisons with measurements in numerical simulations may indicate which barrier shapes better describe halo formation.

Figs 1 and 2 show that the effect of $\mathcal{G}(s, b)$ is small compared to the effects of including the scale dependence of σS_3, and the effect of using different barrier shapes. Therefore, it is a good approximation to set

$$f(s, b) \approx f_0(s, b) \left[1 + \frac{\sigma S_3}{6} H_3\left(\frac{b}{\sqrt{s}}\right)\right]. \tag{31}$$

When the barrier is constant, $b = \delta_c$, then this reduces to the expression presented by Lo Verde et al. (2008). Our analysis shows that there is an additional correction factor which their derivation missed [our factor of $(\sigma S_3/6)\, G$], but that this happens to be small. On the other hand, they include a term which comes from the scale dependence of $\partial\, (\sigma S_3/6)/\partial \ln s$ which we are ignoring (we have checked that it is small.).

4 DISCUSSION

We showed how the excursion set approach may be extended to model halo abundances when the initial conditions were non-Gaussian. In this approach, the estimate of halo abundances is related to the first crossing distribution of a suitably chosen barrier by a suitably chosen set of walks. The physics of collapse set the barrier shape, and the statistics of the initial fluctuation field set the properties of the ensemble of walks: for example, how steps in a given walk are correlated and whether the walks are independent of one another. Our analysis assumes that the steps in a walk are uncorrelated, and the appropriate ensemble contains all possible independent walks. The first assumption may be well motivated only for Gaussian random fields – we argue that it may remain a useful approximation for weakly non-Gaussian fields. The second assumption ignores the fact that averaging over the full ensemble of uncorrelated walks is only an approximation to the more physically appropriate ensemble described in Sheth et al. (2001). Previous work suggests that this allows one to write down simple analytic expressions which are reasonably accurate.

Our analysis was done in two steps – the first showed how the calculation depends on the physics of collapse: spherical and triaxial collapse models are associated with 'constant' and 'moving' barriers (Section 3). For Gaussian initial conditions, our results clarify the nature of approximations made in previous studies of the moving barrier model (see Section 3.3).

For non-Gaussian initial conditions, our analysis assumes that the correlated nature of the steps (in non-Gaussian models) changes the step-size distribution in a calculable way, but that steps are otherwise independent. For weak non-Gaussianity, we approximate the change to

the step sizes by using the Edgeworth expansion (equations 6 and 7). This is not strictly correct – it is an approximation which may be accurate for weakly non-Gaussian fields. (In this context, our analysis of the constant-barrier model showed that previous work on this problem, which made the same assumptions as we do, had missed some terms. However, these turn out to be small.) As we were completing this work, Maggiore & Riotto (2009) presented a very different analysis of the constant-barrier problem which yields consistent results, suggesting that our neglect of the additional correlations between steps associated with $f_{\rm nl} \neq 0$ is reasonable.

Ours is the first analysis of the moving barrier problem for non-Gaussian models: the moving barrier yields quantitatively different predictions for halo abundances than does the constant-barrier model, at a level that current simulations should be able to detect. This is explored further in Lam, Sheth & Desjacques (2009). So, we hope that our results will benefit problems which use halo abundances to constrain the nature of the initial fluctuation field. They also provide a key ingredient to the halo model interpretations of how galaxies cluster (Cooray & Sheth 2002).

ACKNOWLEDGMENTS

We would like to thank the anonymous referee for a helpful report.

REFERENCES

Afshordi N., Tolley A. J., 2008, Phys. Rev. D, 78, 123507
Bond J. R., Cole S., Efstathiou G., Kaiser N., 1991, ApJ, 379, 440
Buchbinder E. I., Khoury J., Ovrut B. A., 2008, Phys. Rev. Lett., 100, 171302
Carbone C., Verde L., Matarrese S., 2008, ApJ, 684, L1
Cooray A., Sheth R., 2002, Phys. Rep., 372, 1
Dalal N., Doré O., Huterer D., Shirokov A., 2008, Phys. Rev. D, 77, 123514
Desjacques V., Seljak U., Iliev I. T., 2009, MNRAS, 396, 85
Grossi M., Branchini E., Dolag K., Matarrese S., Moscardini L., 2008, MNRAS, 390, 438
Grossi M., Verde L., Carbone C., Dolag K., Branchini E., Iannuzzi F., Matarrese S., Moscardini L., 2009, preprint (arXiv:0902.2013)
Hikage C., Matsubara T., Coles P., Liguori M., Hansen F. K., Matarrese S., 2008, MNRAS, 389, 1439
Izumi K., Soda J., 2007, Phys. Rev. D, 76, 083517
Kamionkowski M., Verde L., Jimenez R., 2009, J. Cosmology Astroparticle Phys., 1, 10
Khoury J., Piazza F., 2008, preprint (hep-th/0811.3633)
Komatsu E. et al., 2009, ApJS, 180, 330
Kotz T., Balakrishnan N., Johnson N. L., 2000, Continuous Multivariate Distributions, Vol. 1, Models and Applications. John Wiley & Sons, New York
Koyama K., Soda J., Taruya A., 1999, MNRAS, 310, 1111
Lacey C., Cole S., 1993, MNRAS, 262, 627
Lam T. Y., Sheth R. K., 2009, MNRAS, 395, 1743
Lam T. Y., Sheth R. K., Desjacques V., 2009, MNRAS, in press (arXiv:0905.1706)
Lo Verde M., Miller A., Shandera S., Verde L., 2008, J. Cosmology Astroparticle Phys., 4, 14
McDonald P., 2008, Phys. Rev. D, 78, 123519
McEwen J. D., Hobson M. P., Lasenby A. N., Mortlock D. J., 2008, MNRAS, 388, 659
Maggiore M., Riotto A., 2009, preprint (arXiv:0903.1251)
Maldacena J., 2003, J. High Energy Phys., 5, 13
Matarrese S., Verde L., 2008, ApJ, 677, L77
Matarrese S., Verde L., Jimenez R., 2000, ApJ, 541, 10
Press W. H., Schechter P., 1974, ApJ, 187, 425
Scoccimarro R., Sefusatti E., Zaldarriaga M., 2004, Phys. Rev. D, 69, 103513
Sefusatti E., Komatsu E., 2007, Phys. Rev. D, 76, 083004
Sheth R. K., 1998, MNRAS, 300, 1057
Sheth R. K., Tormen G., 2002, MNRAS, 329, 61
Sheth R. K., Mo H. J., Tormen G., 2001, MNRAS, 323, 1
Silvestri A., Trodden M., 2008, preprint (arXiv:0811.2176)
Slosar A., 2008, J. Cosmology Astroparticle Phys., 03, 004
Slosar A., Hirata C., Seljak U., Ho S., Padmanabhan N., 2008, J. Cosmology Astroparticle Phys., 8, 31
Taruya A., Koyama K., Matsubara T., 2008, Phys. Rev. D, 78, 123534
Valageas P., 2009, preprint (arXiv:0906.1042)
Yadav A. P. S., Wandelt B. D., 2008, Phys. Rev. Lett., 100, 181301

APPENDIX A: APPROXIMATION FORMULA FOR σS_3

The quantity σS_3 measures the strength of non-Gaussianity in the smoothed field. Unfortunately, it requires the computation of several numerical integrals. We have found that the following provides a good approximation:

$$\sigma S_3 \approx 12\, f_{\rm nl} \frac{\langle \delta_R \phi_R \rangle}{\sigma} \left(1 + \frac{1}{6}\frac{{\rm d}\ln\langle \delta_R \phi_R \rangle}{{\rm d}\ln r}\right) \left\{1 - \left[\frac{\sigma}{\sigma(r_0)}\right]^{m_1}\right\} + \sigma S_3(r_0) \frac{\langle \delta_R \phi_R \rangle / \langle \delta_R \phi_R \rangle(r_0)}{\sigma/\sigma(r_0)} \left[\frac{\sigma}{\sigma(r_0)}\right]^{m_2}, \quad \text{(A1)}$$

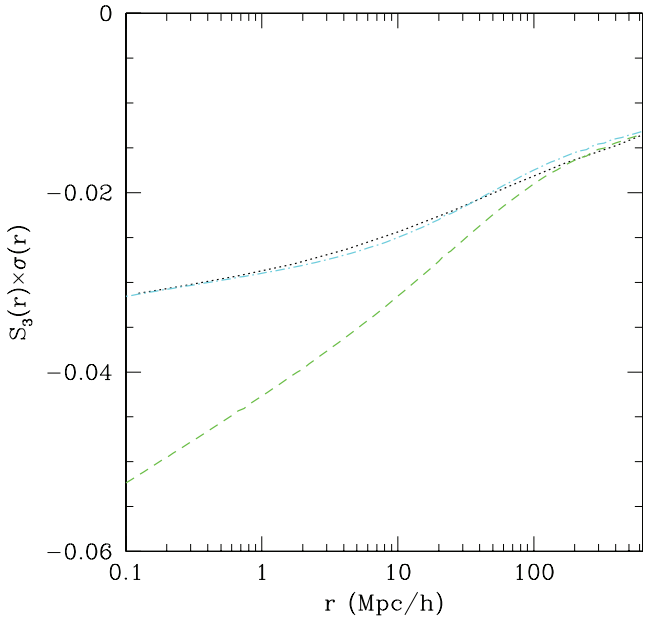

Figure A1. The quantity $\sigma S_3(r)$ for $f_{\rm nl} = 100$. Dotted (black) curve is the numerical result, dot–dashed (cyan) curve is equation (A1), and dashed (green) curve is the approximation from Scoccimarro et al. (2004), which is only expected to be valid on large scales.

where the first term on the right-hand side is the large-scale approximation given in Scoccimarro et al. (2004). If we set $r_0 = 0.1$ Mpc h^{-1}, $m_1 = 0.5$, $m_2 = 0.7$ then $\sigma S_3(r_0) = -0.0316$, and equation (A1) is rather accurate (see Fig. A1).

APPENDIX B: HALO ABUNDANCES IN THE CONSTANT-BARRIER MODEL WHEN $F_{\rm NL} \neq 0$

The main text considered the general case of a moving barrier. When the barrier is constant then it is convenient to define

$$G_{\rm mn} \equiv \int_0^\infty {\rm d}\delta\; p_0(\delta+\delta_c, s; \delta_c, S) h_{\rm mn}\left(\frac{\delta+\delta_c}{\sqrt{s}}, \frac{\delta_c}{\sqrt{S}}, \sqrt{\frac{S}{s}}\right), \tag{B1}$$

making

$$G_{30} = -\frac{\sqrt{s-S}}{\sqrt{2\pi}\sqrt{s}}, \qquad G_{03} = \frac{\left(\delta_c^3 - 3S\delta_c\right)(s-S)^2}{2s^2S^{3/2}} - \frac{\sqrt{s-S}[S(2S-3s)+3\delta_c^2(s-S)]}{\sqrt{2\pi}s^2\sqrt{S}},$$
$$G_{21} = \frac{\sqrt{S}\sqrt{s-S}}{\sqrt{2\pi}s} \qquad \text{and} \qquad G_{12} = \frac{-sS(s-S)+\delta_c^2(s-S)^2}{\sqrt{2\pi}Ss^{3/2}\sqrt{s-S}}. \tag{B2}$$

In addition,

$$G_3 \equiv \int_0^\infty {\rm d}\delta\; p_0(\delta+\delta_c, s; \delta_c, S) H_3(\delta_c/\sqrt{S}) = \frac{\left(\delta_c^3 - 3S\delta_c\right)}{2S^{3/2}}, \tag{B3}$$

so

$$\int_0^\infty p(\delta+\delta_c, s|\delta_c, S) = \frac{1}{2} + \frac{\lambda_{30}}{6}\frac{G_{30}s^2}{(s-S)^2} + \frac{\lambda_{03}}{6}\left[\frac{\sqrt{S}(3s-2S)}{\sqrt{2\pi}(s-S)^{3/2}} - \frac{3\delta_c^2}{\sqrt{2\pi}\sqrt{S}\sqrt{s-S}}\right] + \frac{\lambda_{21}}{2}\frac{G_{21}s^2}{(s-S)^2} + \frac{\lambda_{12}}{2}\frac{G_{12}s^2}{(s-S)^2}. \tag{B4}$$

If the scale dependence of σS_3 can be ignored then $\lambda_{\rm mn} = \sigma S_3$, so, to first order in σS_3,

$$\int_0^\infty p(\delta+\delta_c, s|\delta_c, S) = \frac{1}{2} + \frac{1}{\sqrt{2\pi}}\frac{\sigma S_3}{6}E(s,S), \qquad \text{where} \quad E(s,S) = \frac{2(-2s^{3/2}+3s\sqrt{S}-S^{3/2})}{(s-S)^{3/2}} + \frac{3\delta_c^2(\sqrt{s}-\sqrt{S})}{S\sqrt{s-S}}. \tag{B5}$$

Note that $E(s, S) = 0$ when $s = S$, so when σS_3 is a constant then

$$\frac{\partial}{\partial s}\int_{\delta_c}^\infty {\rm d}\delta\; p(\delta, s) = \frac{f(s,\delta_c)}{2} + \frac{1}{\sqrt{2\pi}}\frac{\sigma S_3}{6}\int_0^s {\rm d}S\; f(S,\delta_c)\frac{\partial E}{\partial s}, \quad \text{where} \quad \frac{\partial E}{\partial s} = \frac{3}{2s}\sqrt{\frac{S}{s}}\frac{\left(\delta_c^2/S\right)(1+\sqrt{S/s})-2}{\sqrt{(1-S/s)}(1+\sqrt{S/s})^2}. \tag{B6}$$

The main text assumes that the second term on the right-hand side is negligible compared to the first. In the approximation where σS_3 is constant, this makes $f(s, \delta_c) = f_0(s, \delta_c)\,[1 + (\sigma S_3/6)\,H_3(\delta_c/\sigma)]$. To see if this is accurate one can substitute this expression for $f(s, \delta_c)$ into

the integral, and check that this contribution really is negligible compared to the first term, $f(S,\delta_c)/2$. Namely, write

$$\frac{\partial}{\partial \ln s}\int_{\delta_c}^{\infty} {\rm d}\delta\; p(\delta,s) = \frac{sf(s,\delta_c)}{2}\left[1+\frac{2}{\sqrt{2\pi}}\frac{\sigma S_3}{6}\int_0^s \frac{{\rm d}S}{S}\,\frac{Sf(S,\delta_c)}{sf(s,\delta_c)}\,\frac{\partial E}{\partial \ln s}\right], \tag{B7}$$

then note that, to leading order in σS_3, we may approximate $f(S,\delta_c)\approx f_0(S,\delta_c)$, so the second term in square brackets is

$$G(s) = \frac{2}{\sqrt{2\pi}}\frac{\sigma S_3}{6}\int_0^s \frac{{\rm d}S}{S}\,\frac{Sf_0(S,\delta_c)}{sf_0(s,\delta_c)}\,\frac{3}{2}\sqrt{\frac{S}{s}}\,\frac{\left(\delta_c^2/S\right)(1+\sqrt{S/s})-2}{\sqrt{(1-S/s)}(1+\sqrt{S/s})^2} = \frac{\sigma S_3}{2}\int_0^1 \frac{{\rm d}x}{x}\,\frac{{\rm e}^{-\left(\delta_c^2/2s\right)(1/x-1)}}{\sqrt{2\pi}}\,\frac{\left(\delta_c^2/s\right)(1+\sqrt{x})-2x}{x\sqrt{1-x}(1+\sqrt{x})^2}. \tag{B8}$$

This paper has been typeset from a TEX/LATEX file prepared by the author.